Preliminary Conceptual Design of a Tokamak Reactor

Fusion Feasibility Study Team

November 1972

UWFDM-36

Preliminary Conceptual Design of a Tokamak Reactor

Fusion Feasibility Study Team

Fusion Technology Institute
University of Wisconsin
1500 Engineering Drive
Madison, WI 53706

http://fti.neep.wisc.edu

November 1972

UWFDM-36

PRELIMINARY CONCEPTUAL DESIGN OF A TOKAMAK REACTOR

by

M.A. Abdou
R.W. Boom
M.W. Carbon
R.W. Conn
J.M. Donhowe
L.A. El-Guebaly
G.A. Emmert
H.K. Forsen
W.A. Houlberg
J.H. Kamperschroer
D.W. Kerst
D. Klein

G.L. Kulcinski
C.W. Maynard
D.G. McAlees
A.T. Mense
P.A. Sanger
W.E. Stewart
I.N. Sviatoslavsky
D.K. Sze
W.F. Vogelsang
W.R. Winter
T.A. Yang
W.C. Young

November 1972

University of Wisconsin

Madison, Wisconsin 53706

FDM 36

PRELIMINARY CONCEPTUAL DESIGN OF A TOKAMAK REACTOR

M.A. Abdou, R.W. Boom, M.W. Carbon, R.W. Conn, J.M. Donhowe, L.A. El-Guebaly, G.A. Emmert, H.K. Forsen, W.A. Houlberg, J.H. Kamperschroer, D.W. Kerst, D. Klein, G.L. Kulcinski, C.W. Maynard, D.G. McAlees, A.T. Mense, P.A. Sanger, W.E. Stewart, I.N. Sviatoslavsky, D.K. Sze. W.F. Vogelsang, W.R. Winter, T.A. Yang and W.C. Young

Table of Contents

I. Introduction

The University of Wisconsin group studying CTR feasibility is now considering a D-T fueled low-β toroidal reactor and we have considered enough of the detailed problems to give a preliminary design. The design philosophy has been to be technically conservative so that the system specified could be constructed using existing technology. The system has not, however, been systematically optimized and this, coupled with the conservatism, makes the system appear expensive. However, the consequences of alternative assumptions are given in a separate section near the end of the paper; and it is noted that there is a wide range of performance that can be predicted with seemingly slight changes in the plasma constraints.

II. Overview of the Total System

The proposed reactor is classed as a low-β Tokamak-like system. This system was chosen primarily because recent advances give the hope for magnetically confined systems that the Tokamak will be able to demonstrate scientific feasibility for fusion. The main structural material is stainless steel. This choice requires that the operating temperature of the coolant, lithium, be held below 500° C because of corrosion considerations. This economic penalty is counterbalanced by the availability of an industry capable of producing high quality, low cost (compared to refractory metals), fabricated components. It is also the only construction material which has extensive radiation effects data available in the anticipated range of CTR operation. Graphite has been chosen as a neutron reflecting material. The superconductor for the magnets is NbTi, which fixes the maximum magnetic field available. Preliminary results indicate the magnets will be the dominant cost in the system which suggests that a low aspect ratio, A (ratio of major radius to plasma radius) is desirable. At the same time, the blanket, shield, magnet, and

dewar structures limit A to the order of three or greater for reasonable fields and volumes. The actual ratio is five. The number of individual magnets used in the system is twelve. This is a compromise between field uniformity, wasted space for cryogenic insulation, and convenience of assembly and maintenance. The aim has been to make the system as modular as possible and thus a system has been designed where the magnets are mounted in pairs for ease of assembly and disassembly. Pumps, headers, and other subsystems are similarly planned in multiples of six or twelve. The system also includes a divertor with the superconducting divertor coils divided into six separate coils as a compromise between the ease of assembly and costs. Figure 1 is a top view of the proposed magnet and divertor coil assembly, while Figure 2 is a cross sectional view showing the D-shaped main magnets, square cross section divertor coils, the central core and the base used to support the entire structure (including the blanket and shield). The divertor slots, vacuum pumps, and the start up coils in front of the first wall are also shown.

III. Design and Subsystem Details

A. Plasma Parameters

The magnets provide a maximum field of 8.6 tesla and, in this geometry, the resulting field strength at the plasma axis is 5.1 tesla. This suffices to allow an energy and particle balance consistent with confinement and stability limits. The details of the analysis are given in another paper of these proceedings [1]. The main features for our purposes are that the plasma will operate at an ion temperature of 12.4 keV with an average ion density of $0.95 \times 10^{20}/m^3$, which gives an average power density of 0.74 MW/m^3 and a total power of 1140 MW$_t$. The operating condition has been reached by enhancing radiation losses through the addition of 0.8% argon atoms. This primarily increases the bremsstrahlung radiation (which carries away most of the energy) to the first

wall. The enhancement is a factor of ten over normal bremsstrahlung losses without impurities. Fractional burn up would not allow the system to operate in this regime without spoiling the confinement time relative to the theoretically predicted value. Spoiling by a factor of 430 results in a mean ion confinement time of 12.2 seconds and a fractional fuel burn up of 10.6%. These results incorporate constraints on the stability factor, q, and on β_p, the ratio of plasma pressure to poloidal magnetic field pressure. The requirement on q is that it be greater than one at all points and the choice q = 1.5 at the edge of the plasma meets the criterion. While a larger choice of q is acceptable, it would reduce the power level that can be achieved. The β_p has been limited to a maximum value equal to $\sqrt{A}$. This provides, via the bootstrap current, a poloidal field of the magnitude required to hold the steady state plasma without the need for an externally induced plasma current.

The steady state operating point obtained in the present instance is thermally unstable; or in the terminology of reactor engineering, the plasma has a positive temperature coefficient. This means any small perturbation from the equilibrium operating point will result in changes that will drive the system further from the equilibrium. In practice, this means that one either seeks a new equilibrium condition which is energetically stable or seeks to feedback stabilize the plasma by external means. It should be possible in principle to obtain another equilibrium point which is stable at some higher ion temperature. The loss mechanisms used to date have the wrong temperature dependence to achieve this, at least at temperatures that are acceptable from the confinement standpoint. Synchrotron radiation and Bohm diffusion have the proper dependence and are being investigated, but

their magnitude and scaling are far from ideal for our purposes. Table I
with further relevant plasma parameters is taken from reference [1].

B. Divertor and Vacuum System

The maximum flux of plasma particles to the first wall is 1×10^{15} cm^{-2} sec^{-1}.
This flux is approximately 45% 12 keV D, 45% 12 keV T, and 10% 10-100 keV He ions.
These values will be reduced by a factor of 10-100 by the use of a divertor.
The heating and surface damage to the wall will be considered in later sections.
However, it is appropriate to discuss here the mechanisms for reducing the flux
to the wall and the consequent effects this may have on plasma operation. Two
schemes have been proposed to partly protect the wall. The first is to maintain
a cold gas in a narrow region between the wall and the plasma. The second is
to utilize a divertor which can remove plasma particles from a zone near the
first wall before they actually strike the wall. This latter scheme has been
pursued in this study.

It is not clear at this time whether or not low-β toroidal reactors
really require divertors. A better understanding of impurity transport and
radiation in plasmas, alpha particle slowing down and transport in bounded
plasmas, and neutral gas effects near the wall, is required to assess the need
for divertors. One must also consider the effects of divertors on the plasma
thermal balance during start up and quench, and, of course, their effect on
economics. The Wisconsin design includes a divertor pending further study
of these points.

The divertor, shown in Figure 2, is of the poloidal type which will
minimize perturbations in the axisymmetric property of the Tokamak. The
poloidal magnetic field is generated by the plasma current and by superconducting
coils outside the blanket and shield. The plasma boundary is the separatrix

between magnetic field lines which surround only the plasma current and those which also pass through the divertor coils. These coils also provide the necessary vertical magnetic field [2] for radial equilibrium and for radial and vertical stability of the plasma. Because the penetration time through the blanket is long, the magnetic field of the superconducting coils will not be able to respond rapidly enough to follow the plasma current during the start up of the discharge. Consequently, the superconducting coils will be operated D C , and their magnetic field will be bucked out during the initiation of the discharge by normal coils inside the first wall. The currents in these coils will go to zero as soon as the plasma is at full current. They will draw power only for 10-50 msec during each burn.

The divertor coils are in 6 modular units, as shown in Figure 1, and are designed so that they are not coupled to the primary coils which produce the plasma current. Thus, the changing magnetic flux through the center of the torus does not change the divertor currents.

The particles diffusing out of the plasma cross the separatrix and travel through the slots along the total magnetic field ($\vec{B}$ toroidal plus $\vec{B}$ poloidal) to a wetted lithium surface where they are buried in the lithium [3] and pumped out of the system by circulation of the lithium. The lithium is in the form of a thin film flowing down a flat surface. At a lithium temperature of $600\,^{\circ}K$, the trapping efficiency exceeds 90% [3] and a residence time in the charged particle beam of 15 sec is short enough to prevent saturation of the surface. The energy input to the surface by charged particles conducts through the lithium film and is removed by standard techniques from the back side of the flat plate. The lithium will contain a high concentration of tritium which will be recovered by external processing similar to that for the tritium bred in the blanket.

The divertor slots are 20 cm wide which corresponds to about 4 ion "banana" widths. This should be sufficient to allow most of the particles to pass through the slot without hitting the walls. Some enhanced erosion of the wall may occur near the neutral point of the poloidal fields because of possible non-adiabatic effects and the fact that flux surfaces come closer to the wall at the neutral point. The curvature of the inside slot in Figure 2 is sufficient to reduce the shielding required to protect the superconducting magnets from neutrons attempting to stream out the slot. The outside slot does not have as much curvature but it "sees" only the edge of the plasma where the neutron production rate is low. Thus, this problem may be manageable. Further refinement in the divertor coil current distribution can increase the curvature of this slot and provide better protection for the superconductors.

The leakage rate of particles out of the plasma (and thus refueling rate) is $\sim 10^{22}$ particles/sec; in order to prevent deterioration of the vacuum, these particles must be removed on a continuous basis. Such a leakage rate represents a gas throughput of 10^3 torr-liters/sec. The neutral gas density in the divertor slots and in the zone surrounding the plasma should be $\leq 10^{-5}$ torr (charge exchange mean free path ≥ 25 meters). This means a total pumping speed of $\sim 10^8$ liters/sec is required. Approximately 90-95% of this is provided by the lithium film in the divertor described above. The remainder is provided by a combination of mercury diffusion pumps and cryogenic pumps backed by Roots blowers and a high capacity roughing pump.

Mercury diffusion pumps have been chosen to avoid the problem of tritium holdup in a fractionating oil diffusion pump. Using currently available hardware, the vacuum pumping system is designed to be compatible with the modular concept. Tucked between each toroidal field magnet coil and the shield

are four 2 x 10^4 liters/sec mercury diffusion pumps and four cryopumps of 2 x 10^5 liters/sec capability in the 10^{-5} torr range.

External to the torus are oil-less Roots blowers and a high capacity forepump. The discharge of the forepump is bottled for deuterium and tritium separation. Tritium holdup in the oil forepump is a recognized but unevaluated problem.

C. Fueling, Heating, and Control

Plasma conditions were considered earlier for steady state operation without reference to the problems of startup and refueling. These problems have not yet been given the same detailed attention as some other aspects of the design.

It is proposed that an initial charge of cold fuel be released in the reaction chamber and that ohmic heating be used to bring the plasma to an ion temperature of about 0.5 keV. The density at this temperature is sufficient to ionize a neutral beam of particles. Neutral beams are then used for a further fueling and heating during the ignition stage.

The neutral beams will be injected through twenty-four ports, each 30 centimeters in diameter, arranged symmetrically around the torus, i.e., two units for each of the twelve magnet sections. Each beam carries an equivalent current of 45 amperes at an energy of 60 keV initially. Using these initial conditions, an energy balance calculation was performed on a unit volume of plasma to obtain estimates of the startup parameters.

After about 5 seconds, the desired ion density (0.95 x 10^{20}/m^3) is reached at an ion temperature of 4.2 keV. The beam currents are then reduced to maintain the desired density. This requires about 9 amperes per injector. The injection energy is still 60 keV so that the neutral beams continue to heat the plasma. After 12 seconds, the density is still constant and the ion temperature

is about 7 keV. At this time, neutral beam injection is discontinued, make-up fuel is supplied at zero energy, and the heatup rate, due soley to alpha particles, is $\sim$1 keV/sec. Heatup continues until a little over 20 seconds when equilibrium is reached at about 12 keV.

For this reactor, the problem of neutral beam penetration into the plasma has not been studied. However, beams with energies up to 1 MeV may be required for uniform penetration under thermonuclear conditions [4]. Further, at equilibrium, injection rates equivalent to about 75 amperes per injector are required to maintain the desired number density. These energy currents include the effects of spoiled confinement. The corresponding injection power requirement is prohibitively large and the injection power would grossly dissrupt the plasma thermal balance. Therefore, a second fueling scheme, such as pellet injection at zero energy, is postulated and put into operation at this time.

The remainder of the startup is controlled by enhancing bremsstrahlung and increasing confinement time spoiling. The equilibrium plasma conditions discussed earlier are reached in about 25 seconds.

We pointed out previously that the equilibrium is thermally unstable. Therefore, a feedback control system is essential. The use of fuel or impurity injection to control the plasma seems difficult. A possibility being considered is the selective excitation and/or de-excitation of plasma instabilities to control the plasma energy balance.

D. Blanket

The key decisions in the design of the blanket are the choice of the structural material and the choice of the coolant. These decisions cannot be made independent of one another because of possible chemical interactions between

the metal and coolant. Our system is an example of this interdependence and it will be evident that one must be willing to make certain trade-offs to build a CTR with "existing" technology.

D. 1. Materials

The choice of 316 stainless steel was made after a consideration of the advantages and disadvantages of this alloy when compared to refractory metals. There are four main advantages for austenitic stainless steels. First is the availability of an extensive industry which is currently producing large, high quality, welded and fabricated nuclear components for the LMFBR program. No such industry presently exists for refractory metals, nor is one likely for many years in the future.

The second reason for choosing stainless steel lies with the existence of detailed design codes which have been developed and tested for the construction of large vessels. Such codes usually require a mature industry and many years of development.

A third reason for this choice is the fact that a large amount of data exists on the response of austenitic stainless steel to high temperature, high fluence neutron irradiation [6-7]. Very little, if any, information is available on such topics as void induced swelling, embrittlement, creep strength or fatigue life of irradiated refractory metals. Another advantage is that the tritium permeability of stainless steel is much lower than that of Nb or V [8-9]. This allows one to more effectively contain the tritium and thus to lower the amount of radioactivity released to the environment. Other reasons for this choice include abundant U.S. reserves of the alloy components (except for Cr), low material costs, easier interfacing with conventional steam systems and heat exchangers, no extremely long lived radioisotopes (i.e. $t_{1/2}^{Max} < 80$ years as opposed to ^{94}Nb which has $t_{1/2} \approx 20,000$ years) and lower vulnerability to metallic transmutation product changes.

Of course, there are some disadvantages to using stainless steel as a structural metal. The major drawback lies with the lower operating temperature required by the poor corrosion resistance of stainless steel to dynamic lithium. This temperature (500° C) is well below that at which the mechanical properties are degraded by temperature (above 650° C).

Although the data on lithium corrosion of stainless steel is limited, it has been shown that penetration rates of >1mm/year have occurred in 316 stainless steel operations in lithium at 650-760° C [10]. This is approximately an order of magnitude higher than is acceptable in the present system. The operating temperature must be lowered to ~500° C in order to achieve <0.1 mm/year corrosion rate values. Hence, the choice of a stainless steel-lithium system imposes a severe penalty on the thermal efficiency of the plant. Detailed economic analysis will be required to see if the total effect of reduced thermal efficiency versus reduced material costs is a positive or negative factor in this system.

Another disadvantage of stainless steel is the high thermal stress induced in the first wall by the absorption of photons and charged particles from the plasma. The magnitude of the stresses can be calculated from the following expression

$$\sigma_{th} = \pm 1/2 \frac{\alpha E}{k(1-\mu)} \left(W_p t + \frac{W_n t^2}{2} \right)$$

where
$\pm$ stands for compression or tension respectively
α = thermal expansion coefficient
E = Young's Modulus
k = thermal conductivity
μ = Poisson's Ratio
t = thickness
W_p = thermal wall loading in Watts/cm^2
W_n = nuclear heating rate, Watts/cm^3

Due to the high thermal expansion coefficient and low thermal conductivity of stainless steel, the stresses in this alloy are usually several times those in equal thicknesses of refractory metals.

An example of the nature of the stresses in a thin walled cylindrial vessel used for this reactor is shown in Figure 3. The hoop stress has been calculated using σ_h = pr/t where p is the pressure and r is the radius of the cylinder. Both thermal and hoop stresses (for p = 700 psi) are shown in Figure 3. The maximum allowable operating stress in the wall is set at 16,000 psi at 500° C using information in the ASME Unfired Pressure Vessel Code. Note that the allowable wall thickness varies from a maximum of 8mm to a minimum of ~2mm.

The first wall thickness was chosen as follows. A corrosion loss of 2mm per 20 years and a sputtering loss of 1mm per 20 years was assumed. The latter value was calculated by assuming a sputtering ratio of 0.01 atoms/ion for 10-20 keV D and T. If the divertor were 90% efficient, the flux of plasma particles to the first wall would be $~10^{14} cm^{-2} sec^{-1}$. No allowance was made for neutron sputtering but the sputtering ratio would probably be less than for energy plasma ions and the total neutron flux would be about the same as for the ions. There was also no allowance made for loss of material via the blistering mechanism [11] as this has not been shown to occur to any great extent in steel at 500° C. However, if the effect is as severe for stainless steel as for Nb, a flux of 10^{13} He ions $cm^{-2} sec^{-1}$ would result in a maximum material loss of ~1mm per 20 years [11-12].

With the above considerations, we have chosen 6mm as the initial thickness and anticipate that ~3mm will still remain after 20 years of operation. If blistering or neutron sputtering become important for this system, one could increase the initial thickness to 8mm.

Two coolant materials were given consideration and the initial conclusions

were at relatively low wall loadings (around 1 MW_t/m^2, power per unit area of first wall) the use of liquid lithium as the coolant is advantageous. At higher wall loadings near 10 MW_t/m^2, the coolant choice would be helium. There is probably a region of overlap where considerations other than pressure and pumping power would be dominant. As our wall loading is at the low end of this range, lithium was chosen as the coolant. Since the blanket requires a lithium-bearing region approximately 50 cm thick to achieve good breeding, it is fortunate that this material is also a suitable coolant. For effective use of the neutrons, a reflector region is also desirable. This is expected to consist of a graphite region about 20 cm thick.

The problems with lithium cooling stem from its electrical conductivity which causes both pressure drops in pumping it across magnetic field lines and a lack of turbulent mixing during flow. The system should be designed to keep the fluid velocities low and to provide temperature equalization in the outgoing lithium. Low velocities are achieved by providing large cross-sections for the flow in the radial and poloidal directions. The modular wall units connected in groups of four are shown in reference [13]. The lithium flows through four modules in series allowing an appreciable total temperature change from inlet to outlet, while the radial flow in each module allows time for conduction equalization of the temperature across the flowing coolant in spite of the lack of turbulent mixing. The headers behind the graphite actually provide lithium for further neutron absorption. At this point, the design is explicit enough to allow detailed nuclear, heat transfer, and materials calculations to take place.

D. 2. <u>Neutronics and Photonics</u>

A one dimensional representation, shown in Figure 4, utilizing homogenized regions is employed for flux calculations. The neutronics and photonics

calculations were carried out using the ANISN computer program [14] and ENDF/B III data. The S_6 approximation with P_3 scattering anisotropy in 100 neutron energy groups was chosen for neutron fluxes and S_6, P_3 scattering, with 43 energy groups was used in treating the gamma fluxes as has been previously found adequate. The calculations give the tritium breeding ratios shown in Table 2. As usual with these one-dimensional representation studies, the breeding is more than adequate. In a calculation on the standard blanket, the breeding was actually slightly higher in stainless steel than in a niobium system despite the fact that stainless steel has a lower (n,2n) cross section. The implication is that the triton from the Li^7 (n, n')α reaction is more important than the extra neutron from an (n,2n) reaction.

The Kerma factors required for energy deposition calculations have been calculated from the ENDF/B III nuclear data files using the computer program MACK [15]. A comparison of these factors for stainless steel and the refractory metals is shown in Figure 5. The data on which this is based are incomplete; thus, while these are considered to be the best values available, they contain considerable uncertainties. This can be seen by noting that the curves in Figure 5 imply that the heating rate in molybdenum will be lower, for the same flux, than in the other materials. However, it is known that the data sets for molybdenum contain no cross sections for charged particle production and thus this contribution is not included in these results. It is expected that their inclusion would make the results much more comparable, since about 65% of the 14 MeV Kerma factors in niobium and iron comes from charged particle reactions.

The neutron heating per material type and by region is given in Table 3. In the first wall, the heating rate is a factor of three greater than would have occurred in niobium. However, the dominant gamma heating is only slightly increased so that the total first wall heating is modestly increased compared to niobium. The total heating as a function of distance from the vacuum is

shown on Figure 6 and is down by two orders of magnitude after 90 cm.

D. 3. Heat Removal

There was originally some doubt as to the viability of lithium cooling due to the strong interaction of the liquid metal and the magnetic fields. The relatively low wall loading of this system is important in this regard.

In designing coolant channels, two design guidelines have been kept in mind. The value of $\vec{v} \times \vec{B}$ was kept a minimum, i.e., the velocity in the directions normal to the field was kept small. The second consideration was to achieve high heat transfer effectiveness by passing all the coolant close to the first wall and segregating the hot and cold fluid. For such a design, as shown in reference [13], the pressure drop associated with the end of loop effects and the Hartmann effects for all the channels within the reactor are calculated. The blanket is designed to stand this pressure, as well as the erosion of the lithium.

The total pressure drop of the coolant is 959 psi. The pumping power required is 20.8 MW. Both these figures seem acceptable. The details of the calculations and other results are given by Sze and Stewart [13]. Their paper also indicates areas for further investigation. It is concluded that lithium is a possible choice as the coolant for a D-T reactor, at least at relatively low wall loadings.

D. 4. Radiation Damage

There are three major areas of concern for the neutron induced damage in the CTR blanket, shield and magnets;

A. Mechanical and physical changes to the structural material

B. Dimensional changes in the graphite reflector

C. Degradation of critical properties of superconducting magnet materials.

Another area which must be eventually considered is the effect of surface damage on the stainless steel first wall. However, such analysis must await experimental determinations of the sputtering and blistering behavior at elevated temperatures.

Since there is no data on materials irradiated with high fluences of 14 Mev neutrons one must find a way to use fission reactor information to anticipate the behavior of the materials in a CTR environment. Such an extrapolation should include the effects of both displacement and transmutation damage. A convenient way to compare fusion and fission neutron damage is to calculate the number of atoms theoretically displaced by the different types of irradiation. Such calculations were made using the displacement cross sections of Doran [16] and the neutron flux and energy spectrum from the preceeding neutronic calculations.

The preliminary calculations reveal that the displacement rates in the stainless steel first wall are $\sim$13 dpa (displacements per atom) per year of operation. The total number of dispalcements after a projected 20 year lifetime is $\sim$260 dpa. These values drop to 0.1 dpa per year and 2 dpa for the wall between the blanket and shield (region 7 in Figure 4) and to 2×10^{-7} dpa per year and 4×10^{-6} dpa for the outer wall of the shield. The above dpa values can be converted to fission neutron fluences typical of the core center for EBR-II by the relationship [17]; 7.03 dpa $\simeq 10^{22}$ n cm^{-2} (E > 0.1 Mev).

No stainless steel has been irradiated to the projected 20 year fluence to the first wall of 3.7×10^{23} n cm^{-2} but it has been found that solution treated 316 stainless steel swells about 8% at 450-500° C and 10^{23} n cm^{-2} due to the production of voids [18]. It has been found that cold working the steel by 20% prior to irradiation at the same temperatures reduces the swelling at $\sim$2 $\times 10^{22}$ n cm^{-2} to < 0.2%. The success of such a thermo-mechanical treatment

at higher fluences is not known but on the basis of the information available, it is possible that swelling values of 3-30% might be found in the first wall at the projected end of life. The effect of increased helium or hydrogen production by 5-14 Mev neutrons is also unknown at this time but it is unlikely that these gas atoms will contribute more than a few percent swelling if they collect into bubbles [19]. The swelling values should decrease quite dramatically through the blanket and, even at 500° C, the maximum swelling in the steel at the outer edge of the blanket should be less than 0.1%.

The effect of irradiation on the mechanical properties of the structural materials can be estimated from the HEDL results on austenitic stainless steel irradiated in EBR-II. Fish et. al. [20] found that the yield strength of 304 stainless steel increased by factors of 3 to 4 in the first 10-20 dpa ($1.5-3 \times 10^{22}$ n cm^{-2}) and thereafter remained relatively constant. If one ignores the effect of increased helium content ($\sim$2500 appm after 20 years in the first wall) this information says that the yield strength will increase dramatically during the first year or two of operation but remain relatively constant over the remainder of the reactor lifetime. Such an effect should not hamper the operation of the structural components.

A more serious effect is the loss of ductility of steel irradiated to a high neutron fluence. Again, Fish et. al. [20] have found that the uniform elongation for 304 stainless steel drops from an unirradiated value of $\sim$30% at 480° C to approximately 3% at 15 dpa, 1% at 30 dpa and saturates at approximately 0.5% around 40-50 dpa. Similar information has also been obtained for 316 stainless steel up to 20 dpa [21]. If one translates this information into a chronological description of the behavior of the CTR first wall structural material, it is noticed that the ductility will drop by a factor of approximately 10 within the first year, approach 1% after 3 years and level out at < 1% thereafter. Such low ductilities must

be considered as one of the most severe problems facing the design engineer. The effect of high helium concentrations will probably accelerate this degradation of in service ductility and it might even be anticipated that the first wall will become extremely brittle within the first year, and perhaps even the first few months of operation. The effect of in-reactor creep on this problem remains to be analyzed.

The loss of ductility becomes a less serious problem as one moves through the blanket away from the plasma. The outer blanket wall will probably retain uniform elongations of 5-10% at 500° C even after a 20 year exposure and there should be little change in the shield components.

A rough idea of the magnitude of dimension change in the graphite can be obtained by noting that the displacement rates in the graphite range from 0.08-0.44 dpa/year. At 20 year lifetimes, it is expected [7] that isotropic graphites will shrink less than 1-2% at an operating temperature of 500-600° C. Such values should not be a major concern as fabricated graphites usually contain approximately 10% of voidage initially and the current displacement values are at least a factor of 3-4 away from the runaway swelling values characteristic of graphite [22].

The final concern is the effect of irradiation on the properties of the superconducting magnets. We again attempted to normalize the displacement damage in terms of dpa values by using the displacement cross section of Nb as typical of the NbTi superconductor [23]. The calculated maximum displacement value for 20 years of irradiation, just outside the outer shield wall is 1.8×10^{-6} dpa. Such a value could correspond to approximately 3×10^{15} n cm^{-2} from a typical thermal reactor. It has been found that irradiation to $4.5-7.5 \times 10^{18}$ n cm^{-2} caused 10-50% drops in the critical current in NbTi [24]. However, since equivalent damage in the UW CTR is approximately 10^{-3} of that at which the experiments show detectable effects it is expected that

radiation damage to the superconducting magnets will be of minor concern. Finally, it is interesting to note that there is little to worry about from the transmutation of Nb to Zr by the high energy neutrons leaking into the magnet. It has been calculated that a maximum of 0.0001 appm of the Nb atoms will be converted to Zr over a 20 year lifetime.

In summary, it appears that the most serious irradiation problem for 316 stainless steel will be the loss of ductility during operation while swelling gradients remain a source of potential trouble. These problems are not unique to steel since they are a characteristic of all the structural materials currently proposed for CTR application. It is also noted that the most severe problems are concentrated in the first wall; while outer components of the blanket, shield and magnets should not be seriously affected by the irradiation at the proposed levels.

E. Shield

A shield behind the blanket is required to protect the magnets and cryogenic system. A schematic representation of the shield is shown in Figure 4. This configuration has not been given great attention and certainly no survey studies have been carried out. Nevertheless, it has been found to give satisfactory attenuation of the neutron and gamma fluxes. It includes borated water which can also serve as the shield coolant if necessary. Its cost is not trivial, but this cost is far from dominant and thus should not strongly influence the choice of materials.

The attenuation was found to be satisfactory. The meaning of this statement is as follows. The power P of the system is attenuated by a factor α in the blanket and shield. Most of the remaining energy, i.e. $P\alpha$, is absorbed in the magnets and must be removed by the cryogenic system at a cost of K reactor watts per watt removed at cryogenic temperatures. The fractional power consumed is $K\alpha$. The quantity K is on the order of 300 watts electrical or, very crudely, 1 KW thermal. For a 1,000 MW_t

plant attenuation of 10^6 results in 1 KW of heat deposited in the magnets. This means 1 MW of refrigeration power is required and this is a negligible energy load. On the other hand, the capital costs may not be negligible and the differential costs from shield design changes are expected to make this approximately the right attenuation for the cost balance. In point of fact, it turns out that the attenuation is an order of magnitude better, i.e., the initial power is reduced by 10^{-7}.

F. Magnets

The designed magnets are far bigger than any constructed to date. In addition, their costs are estimated to be the largest single contribution for the reactor and should be carefully assessed. The key problem for magnet design is mechanical stress which determines the technical and economic problems to a large degree.

F. 1.   Main Magnets

The details of our design of these magnets has been given elsewhere [25]. Here, we summarize those features of concern to the system. The magnets are "D" shaped which provides a constant tension winding region without external support and utilizes structural materials efficiently. This also provides space above and below the circular shields for divertor and vacuum equipment. The maximum field is 8.6 tesla corresponding to the maximum field in NbTi superconductors designed thermally to assure a 5.2° K limit on the temperature of the superconductors. The filaments are fully stabilized with copper and the stresses are kept within the elastic range of copper to avoid mechanical hysteresis effects. The conductors are inserted in spiral grooves in "D" shaped forged stainless steel pancakes as shown in Figure 7. The grooves are of constant width and varying depth on each pancake face allowing a linearly tapered winding to be bonded in with fiberglass reinforced epoxy as insulation. The system is prestressed to allow a greater load without exceeding stress limits.

The "D"'s are 1.25 meters thick and have a total height of 17.86 meters. They are suspended from a central ring 12.3 meters tall, 0.46 meters thick and having a 5.79 meter inner radius (see Figure 2). Each magnet consists of 42 discs, each 5 cm thick, separated from each other by 0.635 cm micarta spacers to allow for edge cooling. The stack is compressed by aluminum alloy bolts which are prestressed mechanically and by differential thermal contraction so that magnetic forces cannot completely relieve the tension. Each disc has 32 turns on each side with the 64 turns double wound from a single length of conductor. The total mass of the magnets is 29.5 million pounds and the stored energy is approximately 1.3×10^{11} joules. The pancake design is shown schematically in Figure 5, taken from reference [25] which may be consulted for further details.

F. 2. Divertor Coils

The superconducting coils needed to supply the vertical field for the divertor and the plasma region will be located above and below the shield at radii of 10 m and 13 m from the center of the reactor, as shown in Figure 1. For ease of assembly and removal it was decided that these coils should be constructed of several individual coils clamped together and energized in series. For convenience, the coils are planned as integral parts of the modular structure such that the main magnets, blanket and shield, coils and associated equipment can be removed from the reactor as units for servicing and replacement.

The forces on these coils due to the toroidal magnets and the steady state current in the plasma have been calculated and are found to produce stresses comparable to those in the toroidal magnets. The normal coils, which are located in the plasma region as shown in Figure 2, are used to cancel the vertical field during start up. They are energized slowly but are de-energized very suddenly, and thus cause shock loading on the super-

conducting divertor coils. This shock loading will require additional structural reinforcing in the coil support system. Finally, the cross-over regions are in a 6 tesla toroidal field and carry currents in opposite directions. This produces a repulsive force as well as a bending moment, and these forces must all be reconciled. However, it appears possible to support the coils from the toroidal magnets, which are themselves very massive structural members, if these loads are included in their design.

F. 3. Cryogenic System

The details of the cryogenic plant have not yet been fully studied. The mode of construction would likely continue to be modular with one unit per main magnet.

As it turns out, in the present reactor the shield is overdesigned and the total radiation load to the magnets is reduced to about 100 watts. Future designs will probably not use as thick a shield since this would reduce wall thickness and allow either a smaller magnet or larger plasma volume. The heat load per unit would probably be less than 200 watts and is unlikely to exceed a kilowatt per magnet unit in any design.

The entire system will likely be operated at cryogenic temperatures, but in order to conserve helium, each magnet and divertor coil will have its own liquid helium jacket.

G. Tritium Handling

The choice of the proposed reference design reactor, i.e., 1140 MW_t, stainless steel construction with lithium as a coolant, gives us an opportunity to design a specific tritium removal system. An overall view of the problems associated with tritium removal systems is given by Watson [26]. The results of his analysis suggests that the thin metallic window approach is likely to provide the best chance of attaining a tritium inventory in the blanket at a satisfactory level. However, problems associated with

carbon mass transfer preclude the use of a niobium or palladium window in a stainless steel system and it was decided to investigate an alternative approach using a cooled getter. The design presented here represents a first try and is by no means optimized. Further, the ideas on a modular approach have not been incorporated. Alternative materials must be investigated, the problem treated in a more complete fashion, and the basic assumptions used in the trap design must be re-evaluated. The calculations as reported here, however, do show that it could be possible to provide an adequate removal system at a reasonable cost.

The system chosen is outlined in Figure 8. The lithium from the blanket is passed through an intermediate heat exchanger and its heat transferred to a second lithium loop and then to the main heat exchanger to the steam system. The intermediate loop is used to isolate the steam system from the lithium in the blanket. A portion of the lithium in the first loop is bled off, cooled in the regenerator and passed through a packed bed of getter which absorbs the tritium from the lithium stream. The lithium from the trap is then reheated in the regenerator and returned to the main coolant stream. After the trap has operated for some period of time, it becomes saturated and it is necessary to take it off line for regeneration while the second trap takes over.

The quantities of interest are the inventory of tritium in the primary and intermediate loops, the fraction of the primary loop lithium bled off of the cold trap, and the time required for the trap to load up.

The limit on the amount of tritium which can be tolerated in the lithium loops is set by the allowable loss of tritium into the steam system. This has been taken to be four curies per day. The leakage in turn is determined by the surface areas of the heat exchangers. A thermal design was chosen and a heat exchanger design was based on a 50°C rise in the lithium coolant to an outlet temperature of 500°C for a two loop plant. These calculations

led to an area of 15,000 ft^2 for the main heat exchanger and 16,000 ft^2 for the intermediate heat exchanger.

Using these values with a release rate of 4 Ci/day yields an inventory of .64 Kg/loop or a total of 1.28 Kg.

A mass balance on the tritium inventory gives the following equation

$$I = F(K + I)$$

where

I = fraction of inventory added per pass through the reactor = 4×10^{-4}

K = fraction of tritium removed per pass through the trap

F = fraction of lithium bled from the main stream

The cold trap design follows the treatment of packed beds in Bird, Stewart, and Lightfoot [27]. The getter was chosen to be yttrium at a temperature of 200°C. The basic assumptions include:

1. The trap is initially full of pure lithium,

2. The tritium is removed evenly in the cold trap,

3. The tritium is uniformly distributed in the lithium,

4. The concentration of the tritium absorbed in the sorbent is proportional to the local concentration of tritium in the solution,

5. The concentration of tritium in lithium is small and the resistance of the solid to mass transfer is negligible,

6. And, most importantly, the reaction between the getter and the tritium proceeded fast enough so that chemical equilibrium existed at the lithium-getter interface.

With these assumptions, it was found that each cold trap (four are needed) would have a radius of 1 ft., a height of 2 ft., and would have a time between regnerations of 1 day. Based on a yttrium price of $150/lb, the cost of the getter per cold trap would be $240,000 or ~ $1 million total.

IV. Alternate Design Assumptions

Beta Limit

Since the power scales as $(\beta_p)^2$, one would like to use the largest β_p consistent with long term plasma equilibrium. Two limits on β_p have been discussed in the literature. Shafranov [28] imposes the limit $\beta_p \leq A$ where A is the aspect ratio. At this limit the separatrix between the vertical magnetic field and the poloidal field shrinks to the plasma surface. Larger values of β_p result in the splitting of the magnetic surfaces and a sharp increase in particle energy losses. Galeev and Sagdeev [29] have discussed a different β_p limit for a steady state Tokamak. This limit, $\beta_p^{max} \leq \sqrt{A}$, is a result of the radial particle diffusion giving rise to a "boot strap" current in the longitudinal direction. A larger value of β_p^{max} requires reversed electric fields at the plasma edge which may not be possible to achieve even in a pulsed mode.

Our design has used the more conservative limit $\beta_p^{max} = \sqrt{A}$. If we had chosen to use the limit, $\bar{\beta}_p = A$, all other parameters remaining the same, the power would have been increased by the ratio

$$\left(\frac{\frac{3}{2} A}{\sqrt{A}} \right)^2 = \frac{9}{4} A$$

or approximately a factor of 10 for our case. (The factor of 3/2 arises because $\bar{\beta}_p = 2/3\, \beta_p^{max}$ when $n = n_0 (1 - (r/r_p)^2)^{1/2}$. However, operation at $\bar{\beta}_p = A$ will not be at steady state.

Increased Magnetic Field

The Wisconsin Tokamak superconducting magnets have been designed to operate at 4.2° K (although the superconductor can carry the total design current at 5.2° K). If the refrigeration system capability is improved so that the magnets operate at 3.2° K, the maximum field will increase from 8.5 T to about 10 T. Since the power scales as the fourth power of the

magnetic field, this increase will result in a doubling of the power. The cost, increased structural support and refrigeration, will probably scale as the square of the magnetic field. The net result is more economically attractive than our present design and will be incorporated in our next design iteration.

V. Conclusion

The main conclusions can be summarized as follows: (A) Plasma - A careful and self consistent look at the energy and particle balances in a steady state plasma has been carried out. It is concluded that a satisfactory operating point can be found by using bremsstrahlung enhancement by impurities and invoking confinement spoiling. The operating point is energetically unstable. However, there are potential mechanisms allowing a stable point, but the subject is not satisfactorily resolved at this point. It may also be possible to feedback control the unstable point.

The divertor described here has two slots with the advantages thay a) the slots have enough curvature to reduce the shielding needed behind them, b) the particle flux that must be handled is reduced thus simplifying the exhaust cooling problem, and c) the magnet coils can be moved in closer behind the shield. Also, a vacuum system has been devised which uses existing equipment, indicating that this should be no problem in a reactor. The wetted lithium wall used to stop the exhaust fuel seems technically feasible with a reasonable development program.

Heating the plasma by neutral beam injection presents problems; for while the required beams can probably be achieved today, it is not at all clear that the beams will penetrate the plasma and stay in the confinement region. Pellets remain an unevaluated possibility for fueling after ignition.

It is felt that there exists problems in several areas but these present no major obstacle to reactor feasibility. (B) Materials- A preliminary assessment of expected material problems has been carried out. It appears that the problems of the first wall are still the only ones which pose a serious threat to the feasibility of a fusion reactor. Neutron irradiation will cause swelling which is serious but probably manageable; however loss of ductility is a major problem. In addition, the blistering and sputtering by the charged particle flux to the wall is inadequately assessed and may be very serious. The materials problems consitutes the major challenge to a feasible reactor. (C) Blanket - Neutronics and photonics problems do not appear at this time to be serious. Nevertheless, this area requires further evaluation because data uncertainties will become crucial when a serious effort is made to optimize the system by reducing the blanket and shield thickness.

Heat removal by lithium cooling is expected to be feasible at the wall loadings and magnetic fields given here. At either higher wall loadings or fields this may no longer be true but one can probably cool with helium in that case. No major problems exist in the blanket design. The shielding requirements seem reasonable but considerable further work is desirable to optimize the shield. (D) Magnets- Cryogenic problems are straight forward and within the realm of existing technology, the only comment being that the proposed systems are somewhat larger than current systems. The magnets described here use conventional superconductors and stabilizing techniques. In this sense they are conventional. However, they are far bigger than any in existence and pose mechanical stress and fabrication problems that are new to magnet technology. Proposed solutions to these

problems and it is believed that these would not be a major obstacle to
feasibility.

(E) Safety – Tritium handling will pose some development problems but
they do not seem unconventional enough to become a major obstacle.

At this point no optimization studies have been carried out and these
are definitely needed. In fact, there are indications that factors of two
or more in the economics of the system are readily achievable. While the
work reported here does not examine all of the problems that will be
encountered in constructing a power Tokamak reactor, many of the major
questions have been examined in some detail. Further work is in progress
and a final report will give our most realistic assessment.

Table I

Plasma Parameters

Mc	6.4	τ_c^i	12.2 sec
N_H	10.0	q	1.5
S	430.0	r_p	2.5 m
T_e	11.8 KeV	y	0.9
T_i	12.4 KeV	B_{TO}	5.1 T (on axis)
$\langle \sigma v \rangle$	$1.8 \times 10^{-22} m^3\text{-sec}^{-1}$	B_p	0.68 T
$n_i \tau_c^i$	$1.16 \times 10^{21} m^{-3}\text{-sec}$	T_B	2.25 m
f_b	10.6%	β_p	$\sqrt{5}$
n_i	$0.95 \times 10^{20} m^{-3}$	$\langle P \rangle$	1140 MW_T
n_e	$1.0 \times 10^{20} m^{-3}$	$\langle P/V \rangle$	0.74 $MW/^{-3}$
n_α	$0.25 \times 10^{19} m^{-3}$	Neutron Wall Loading	0.53 MW/m^2
I	8.5×10^6 amps	γ-Wall Loading	0.10 MW/m^2
$\dfrac{n_{im}}{n_i} = .008$		Leakage Power to Divertor	36.60 MW
$Z_{im} = 18$			

Table II

TRITIUM PRODUCTION PER INCIDENT NEUTRON

	T_6	T_7
Zone 4	0.8559	0.5162
Zone 6	0.1280	0.0051
Total	0.9839	0.5213
$T = T_6 + T_7$	1.5052	

Table III

Comparison of Neutron Heating Rates in Units of Watts

On a Per Material and Per Zone Basis

(Source Strength; 10^{14} neut/cm^2-sec)

material / zone	Li^6	Li^7	Graphite	Fe	Cr	Ni	Lead	Total by Zone
3 (SS)				5.4428	1.2357	1.7237		8.4022
4 (95%Li+5%SS)	76.1547	89.0494		5.044	1.1626	1.7185		173.1292
5 (Graphite)			6.0211					6.0211
6 (95%Li+5%SS)	9.9231	1.3572		0.03923	.0094	0.1483		13.3437
7 (SS)				0.1096	0.02708	.0359		0.175258
8 (Lead)							0.02035	0.02035
9 (SS)				0.00511	0.00139	0.001105		0.007605
Total by Material	86.0775	90.4060	6.0211	10.6407	2.4361	3.4940	0.02035	199.096
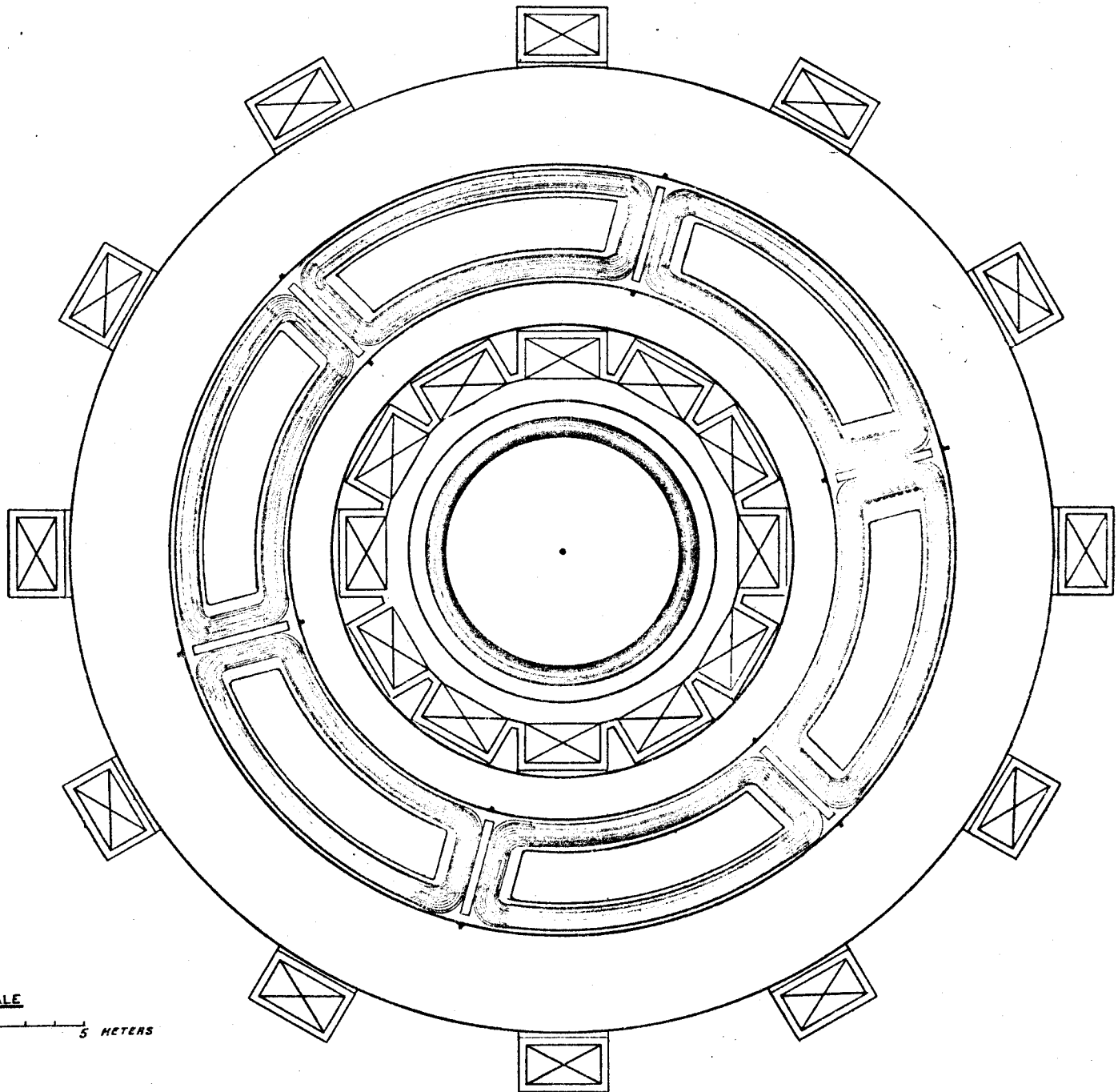
SCALE

0 ————————————— 5 METERS

UNIV. OF WIS. CONCEPTUAL DESIGN FOR A
FUSION
POWER TOKOMAK

UNIV. OF WIS. CONCEPTUAL DESIGN FOR A

FUSION

POWER TOKOMAK

SCALE

0   5   METERS

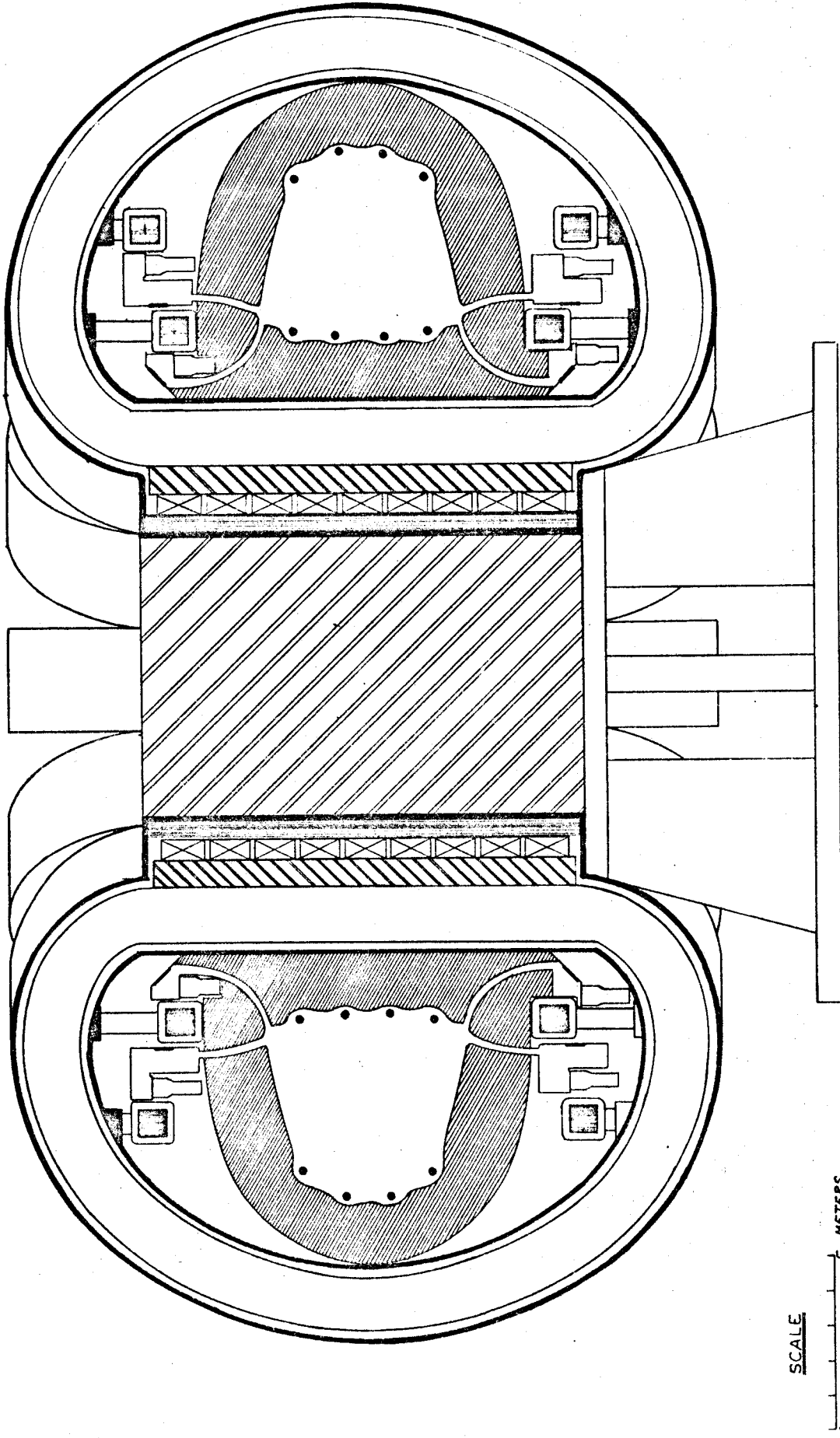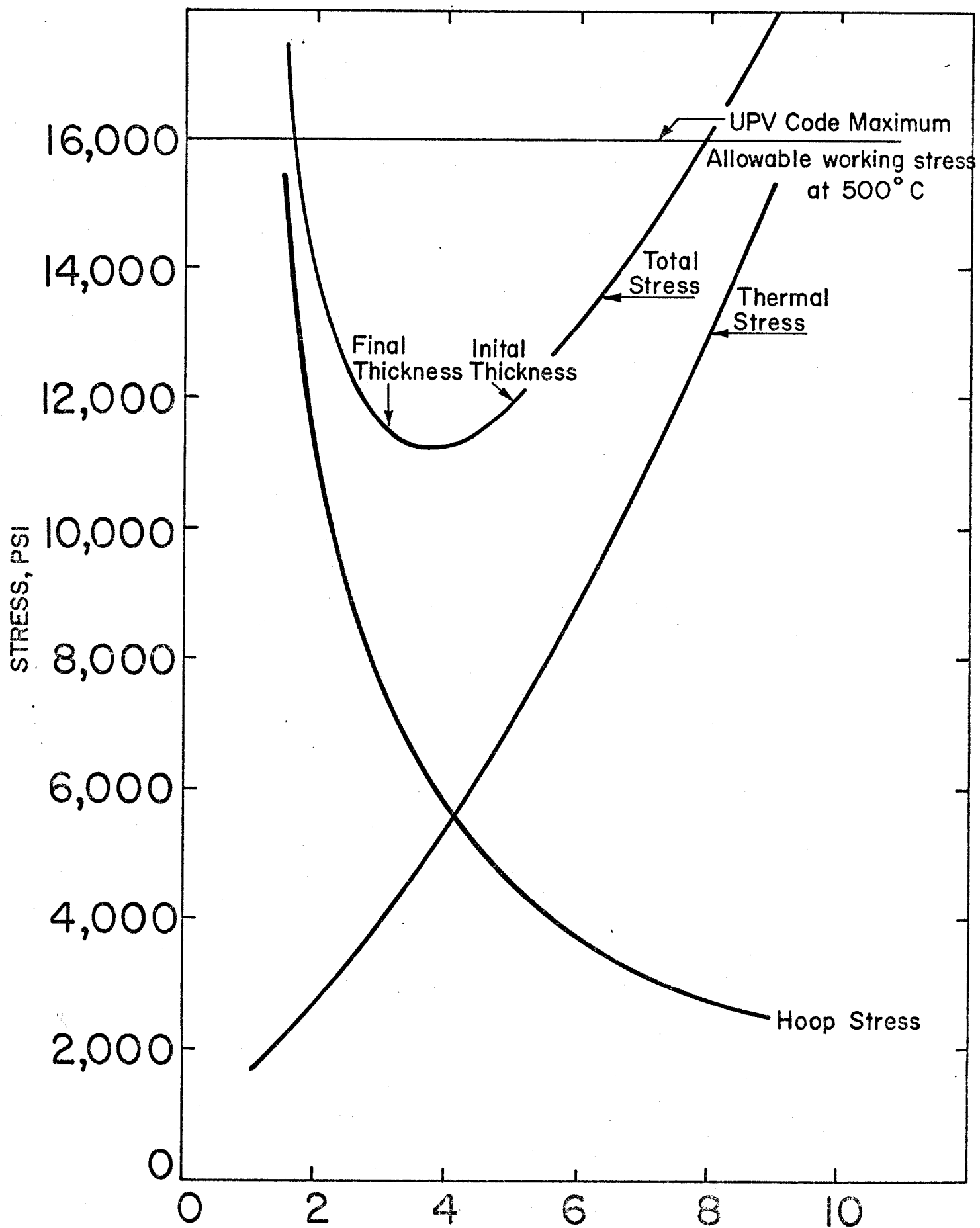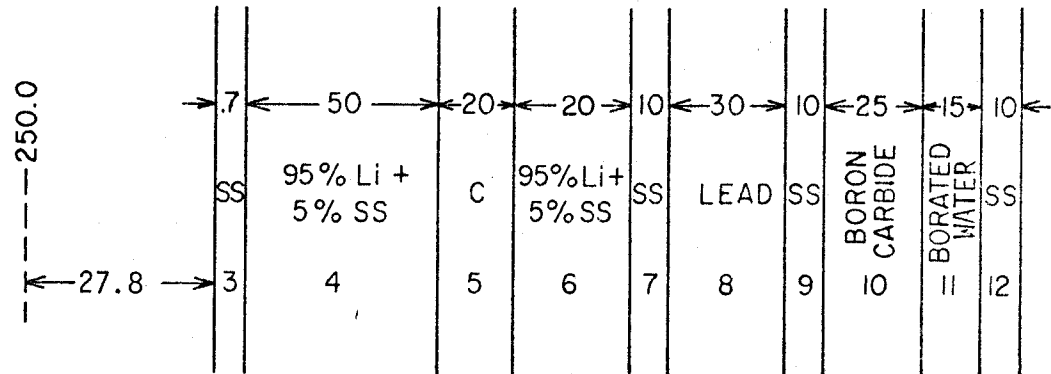# Fig. 3 Stresses in the first wall as functions of wall thickness

Fig. 3 Stresses in the first wall as functions of wall thickness

SCHEMATIC OF BLANKET AND SHIELD

FIGURE 4

KERMA FACTORS COMPARISON
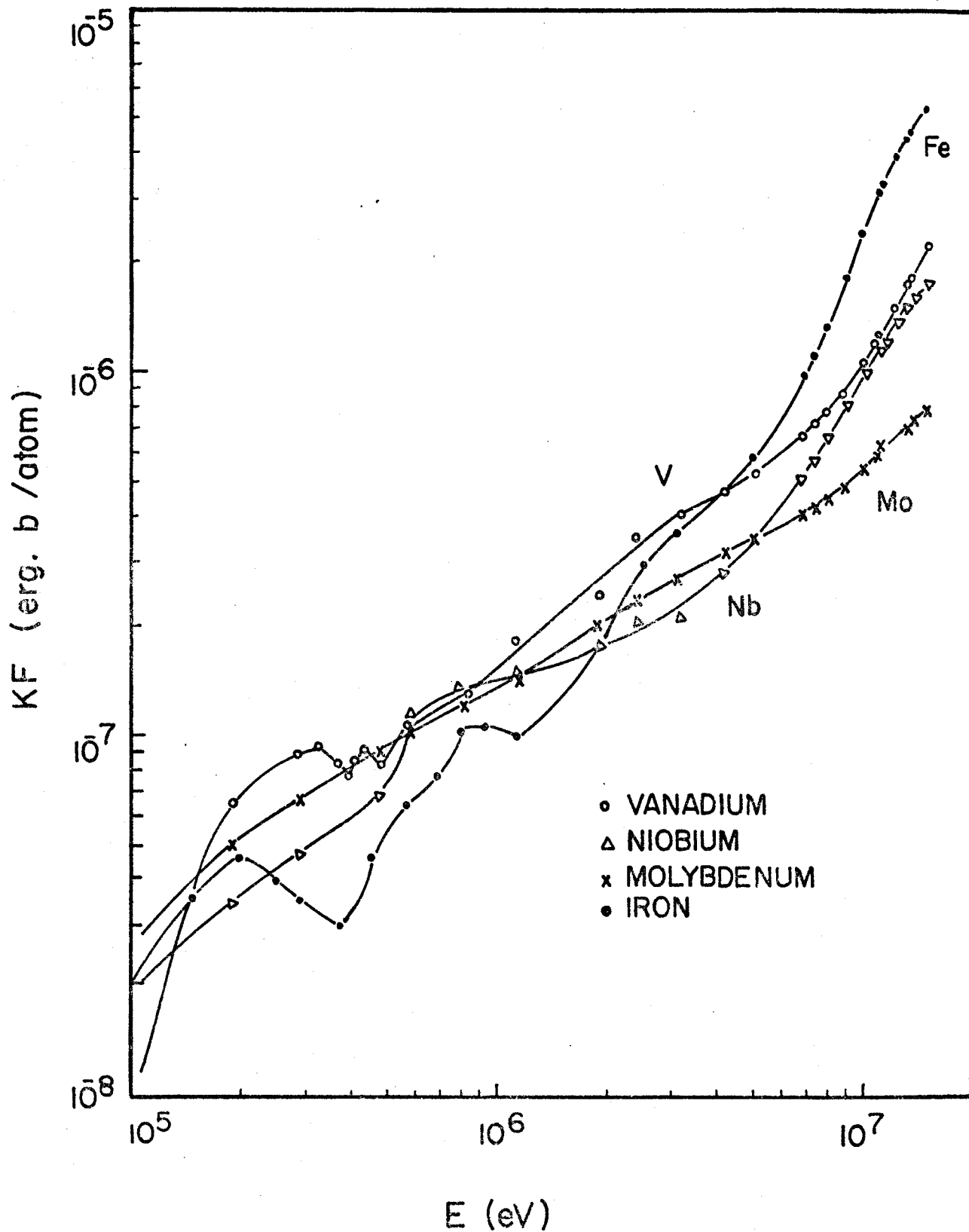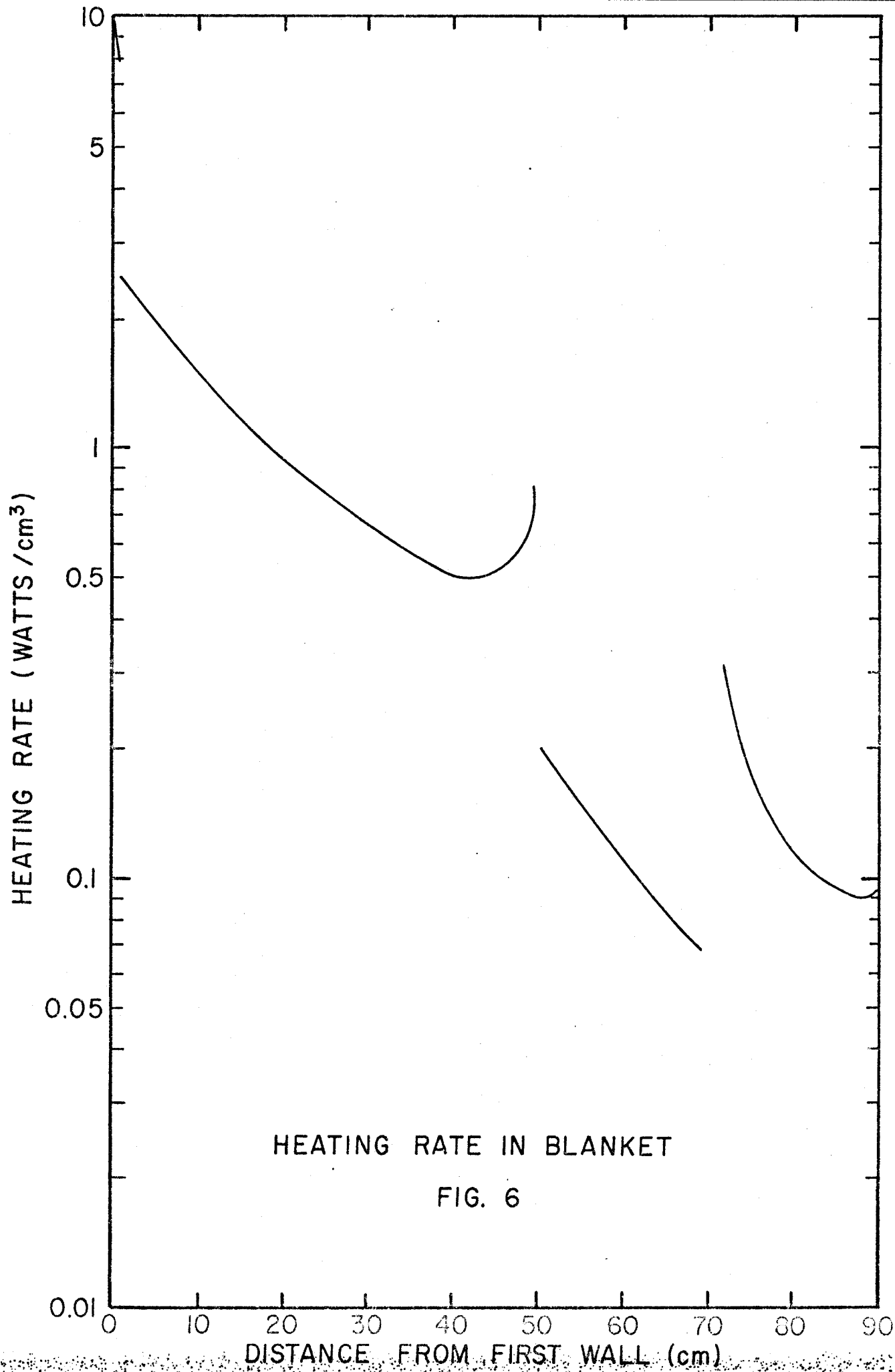FOR FOUR STRUCTURAL MATERIALS OF INTEREST
FOR CTR

FIGURE 5

HEATING RATE IN BLANKET

FIG. 6

PANCAKE MAGNET FORM

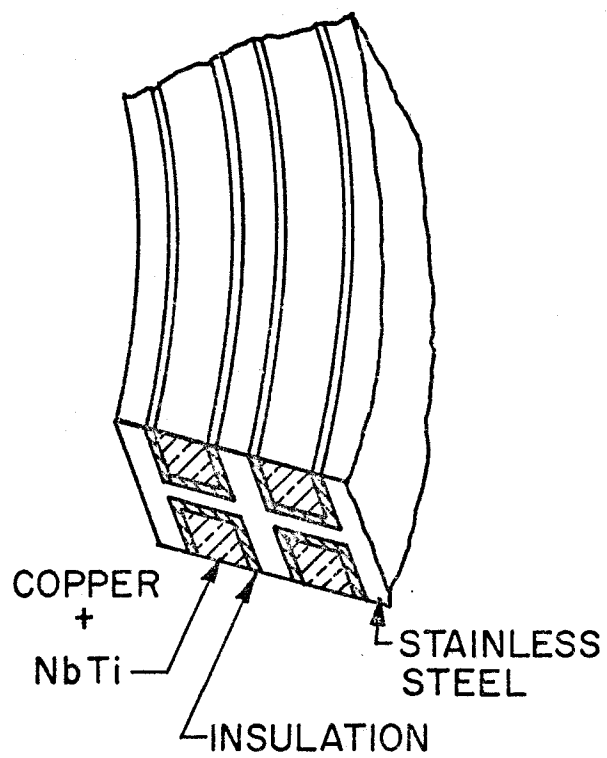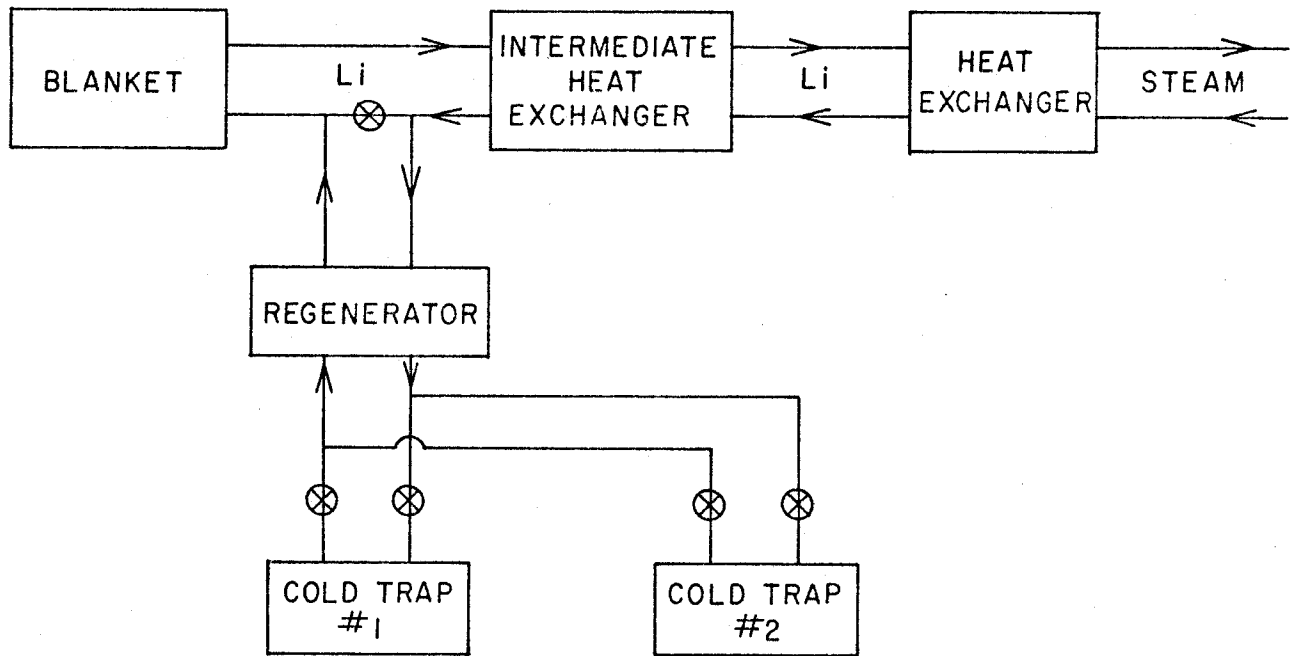
COPPER
+
NbTi

INSULATION

STAINLESS
STEEL

FIGURE 7

TRITIUM REMOVAL SYSTEM BLOCK DIAGRAM

FIGURE 8

References

1. R. W. Conn, D. G. McAlees, G. A. Emmert, "Self-Consistent Energy Balance Studies for CTR Tokamak Plasmas," Texas Symposium, November 1972.

2. V. S. Mukhovatov and V. D. Shafranov, Nuclear Fusion 11, 605 (1971)

3. G. M. McCracken and S. K. Erents, "Ion-Burial in the Divertor of a Fusion Reactor," BNES Nuclear Fusion Reactor Conference at Culham Laboratory, September 1969, p. 353.

4. A. C. Riviere, Nuclear Fusion 11, 363 (1971).

5. J. W. Corbett and L. C. Ianniello, "Radiation Induced Voids in Metals," Proceedings of 1971 Conf., Albany, N. Y., AEC Symposium Series, Number 26.

6. "Effects of Irradiation of Structural Materials", ASTM Conference in Los Angeles, Calif., June 1972, to be published.

7. "Irradiation Embrittlement and Creep in Fuel Cladding and Core Components," British Nuclear Energy Society Conference, London, November 1972, to be published.

8. R. W. Webb, NAA-Sr-10462, July 1965.

9. R.R. Heinrich, C.E. Johnson, and C. E. Crouthamel, J. Electrochem Soc., 112.

10. J. H. Stang, E. M. Simons, J. A. DeMastry, and J. M. Genco, DMIC Report, 227, 1966.

11. M. Kaminsky and S. K. Das, Applied Physics Letters, November 1, 1972.

12. S. K. Das and M. Kaminsky, Applied Physics, January 1973.

13. D. K. Sze and W. E. Stewart, "Lithium Cooling for a Low-β Tokamak Reactor," Texas Symposium, November 1972.

14. W. W. Engle, Jr., "A User's Manual for ANISN," USAEC Report K-1693 (1971).

15. M. A. Abdou, C. W. Maynard, and R. O. Wright, "MACK: A Computer Program to Calculate Neutron-Induced Energy Release Parameters (KERMA) and Multigroup Neutron Reaction Cross-Sections from Nuclear Data in ENDF Format," ORNL-TM-3994, (October 1972).

16.   D. G. Doran, Nuclear Science and Engineering, 49, 130 (1972).

17.   D. G. Doran, HEDL-SA-482, August 1972, to be published.

18.   H. R. Brager and J. L. Straalsund, HEDL-TME72-108,1972.

19.   D. G. Martin, "Nuclear Fusion Reactors," UKAEA, Culham Laboratory, September 1969, p. 399.

20.   R. L. Fish, J. L. Straalsund, C. W. Hunter, and J. J. Holmes, ASTM 1972 Annual Meeting, Los Angeles, June 1972, to be published.

21.   J. J. Holmes, A. J. Lovell, and R. L. Fish, ibid.

22.   W. J. Gray and W. C. Morgan, this conference.

23.   D. G. Doran, to be published.

24.   M. Soell and S. L. Wipf, Applied Superconductivity Conference, Annapolis, 1972.

25.   W. C. Young and R. W. Boom, "Materials and Cost Analysis of Constant-Tension Magnet Windings for Tokamak Reactors," Paper presented at Fourth International Magnet Conference, Brookhaven,September 1972.

26.   J. S. Watson, "An Evaluation of Methods for Recovering Tritium from the Blankets and Coolant Systems of Fusion Reactors," ORNL-TM-3797 (July 1972).

27.   R. B. Bird, W. E. Stewart and E. N. Lightfoot, "Transport Phenomena," Wiley and Sons, 1960.

28.   N. B. Kruskal and R. M. Kulsrud, International Conference on Peaceful Uses of Atomic Energy, (Proc. Second Conference Geneva, 1958) 31, U. N., Geneva (1959) p. 213, and V. D. Shafranov, Zh. eksp.teor. Fiz.37, 1088 (1959).

29.   A. A. Galeev, R.Z. Sagdeev, JETP Lett. 13, 113 (1971).